



29 **Introduction**

30 In recent years, the impacts of global climate change have become increasingly severe,
31 particularly the significant increase in the frequency of various types of extreme weather and
32 climate events (Faranda et al., 2023; Liu et al., 2022; Zhang et al., 2016). The World
33 Meteorological Organization's 2022 report on the state of the climate in Asia shows that the
34 rate of warming in Asia is higher than the global average, with droughts, floods, and
35 heatwaves affecting most parts of the world (State of the Climate in Asia 2022). Severe
36 fluctuations in climatic elements can alter water circulation processes, affect development
37 trends of climate change, and even change the evolutionary patterns of ecological
38 environments. Among these, stable isotopes in precipitation are an excellent comprehensive
39 tracer, playing an important role in revealing water cycle processes, climate change
40 information, and mechanisms of water resource use in ecosystems (Bowen et al., 2019; Wang
41 et al., 2022). Therefore, in the face of increasingly complex climate conditions, we need more
42 comprehensive data on stable isotopes in precipitation at various spacetime scales to help
43 understand climate change phenomena.

44 Stable isotopes in precipitation are intermediate variables in isotope hydrological cycles.
45 They are influenced by factors such as temperature, precipitation, wind speed, relative
46 humidity, and the source of water vapour (Gat, 1996; Jiao et al., 2020). In atmospheric water
47 vapor and precipitation, non-equilibrium fractionation and equilibrium fractionation cause
48 different degrees of variation in $\delta^2\text{H}$ and $\delta^{18}\text{O}$ during phase changes (evaporation,
49 condensation) (Craig, 1961). Fractionation is constrained by surrounding climatic conditions,
50 causing hydrogen and oxygen stable isotopes in precipitation to carry a wealth of climate
51 information in their changes. For example, effects like temperature, precipitation volume, and
52 elevation (Dansgaard, 1964; Ma et al., 2023). The "temperature effect" implies that as
53 temperature increases, the values of $\delta^2\text{H}$ and $\delta^{18}\text{O}$ gradually increase. This effect is the most
54 prevalent influence on stable isotopes in precipitation; spatial "elevation" and "latitude"
55 effects can be attributed to "temperature effects". Moreover, seasonal variations in stable
56 isotopes in precipitation are also temperature-dependent. Rainfall has a more pronounced
57 effect on hydrogen and oxygen stable isotopes in precipitation in low-latitude areas, often
58 associated with abundant precipitation. The deuterium excess ($d\text{-excess} = \delta^2\text{H} - 8 \times \delta^{18}\text{O}$)



59 reflects the source of water vapour and atmospheric moisture conditions, largely affected by
60 relative humidity, with an average deuterium excess of around 10‰ from oceanic water
61 vapour (Dansgaard, 1964). The complexity of influencing factors determines the diverse
62 applications of stable isotopes in precipitation. The signals of hydrogen and oxygen stable
63 isotopes in precipitation can be recorded by geological carriers (ice cores, tree rings, loess,
64 cave stalactites, etc.) (Eastoe and Dettman, 2016). They provide essential archives for
65 describing historical climate change and water cycles, useful for paleoclimate reconstruction,
66 especially the reconstruction of monsoon climates (Caley et al., 2014). Additionally, stable
67 isotopes in precipitation can identify extreme weather events to understand their water vapour
68 sources and mechanisms (Zhao et al., 2023). The composition of hydrogen and oxygen
69 isotopes in precipitation can be used to infer the proportions of plant transpiration water
70 vapour, surface evaporation water vapour, and advection water vapour (Zhu et al., 2019).
71 Spectral remote sensing technology has advanced the capability to obtain large-scale water
72 vapour stable isotope data through satellite inversion (Shi et al., 2022; Wei et al., 2019),
73 deepening the cooperative effect with stable isotopes in precipitation and yielding good
74 results in meteorological and hydrological research in low-latitude regions. Incorporating
75 stable isotopes in precipitation into atmospheric circulation models has improved our
76 understanding of future climate change. Also, coupling stable isotopes in precipitation with
77 hydrological models reduces model uncertainty (Delavau et al., 2017; Nan et al., 2021;
78 Nelson et al., 2021).

79 In 1961, the International Atomic Energy Agency (IAEA) and the World Meteorological
80 Organization (WMO) began establishing the Global Network for Isotopes in Precipitation
81 (GNIP), which is the world's primary observation system. To date, research on stable isotopes
82 in precipitation primarily relies on the GNIP database. However, GNIP's observations are very
83 unevenly distributed in time and space. Global and regional-scale research on stable isotopes
84 in precipitation mainly depends on model simulations. The relationship between predicted
85 data from models and actual measured data is "comparative". Although model simulations can
86 compensate for the absence of measured data and are particularly advantageous in revealing
87 the operating mechanisms of large-scale climate systems and water cycles, existing models
88 for stable isotopes in precipitation are often insufficiently accurate. They cannot check



89 long-term trends or characteristics of interannual variation. By integrating independent data to
90 provide a higher density of data, it's possible to enhance the precision of model simulations.

91 We have compiled precipitation stable isotope data from the Eurasian continent since
92 1961 with the aim of providing more comprehensive data support for the following research
93 areas:

94 Climate research: Precipitation-stable isotopes exhibit geographical and seasonal
95 variations, which can be used to study climate change and the impact of solar radiation. By
96 comparing and analyzing the stable isotopes of precipitation in different regions of the
97 Eurasian continent, long-term climate trends can be revealed, such as changes in precipitation
98 distribution and the evolution of monsoon systems.

99 Earth system research: Precipitation stable isotopes are not only influenced by climate
100 and water cycle but also by geological and biological processes. By integrating precipitation
101 stable isotope data from the Eurasian continent, it is possible to investigate in-depth the
102 interactions between different components of the Earth system, such as the interaction
103 between the atmosphere and the ocean, and the water cycle in terrestrial ecosystems. This will
104 contribute to a better understanding of the functioning and changes of the Earth system.

105 Water cycle research: Precipitation-stable isotopes serve as important indicators of the
106 water cycle and can track the sources, evaporation, and precipitation processes of water. By
107 analyzing the spatial distribution and variations of precipitation stable isotopes on the
108 Eurasian continent, it is possible to understand the processes of water evaporation,
109 precipitation, and recycling, revealing the patterns of water resource distribution and changes.
110 This provides support for water resource management and hydrological modelling.

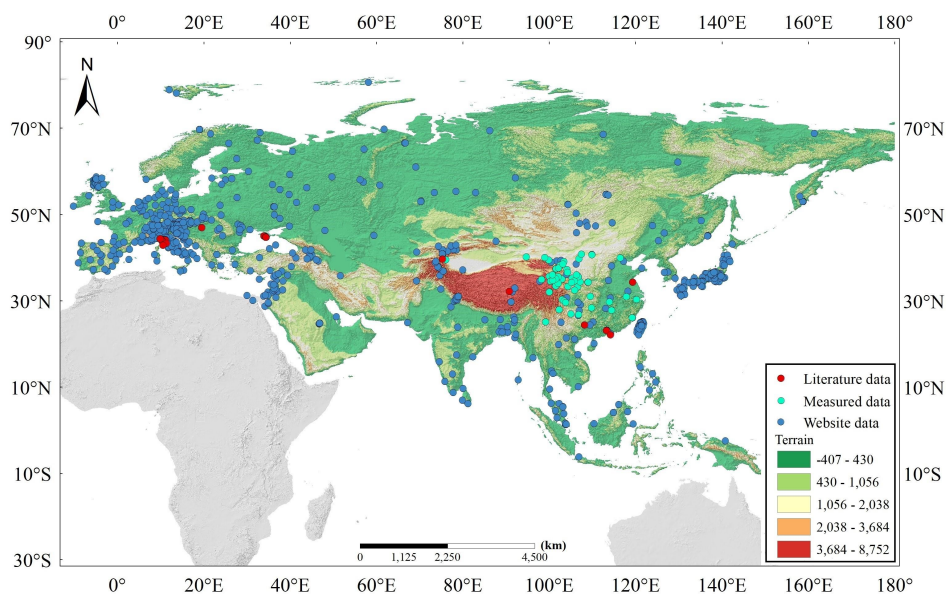
111 Paleoclimate reconstruction: Precipitation-stable isotopes exhibit long-term variations,
112 making them useful for reconstructing past climate changes. By analyzing the chronological
113 sequences of precipitation-stable isotopes on the Eurasian continent, it is possible to study
114 paleoclimate changes and ancient environmental evolution, such as changes in precipitation
115 during ice ages, variations in monsoon intensity, and more. This provides historical references
116 and predictions for understanding modern climate change.

117 **1. Study area**

118 The Eurasian continent (10°45'N - 77°44'N, 9°30'W - 169°45'E) spans a vast territory,



119 with considerable variations in natural geographic conditions within the region (Fig.1).
120 Significant thermal differences between sea and land have given rise to a typical monsoon
121 climate system on the southeast coast, while interactions between Atlantic moisture and
122 planetary wind systems result in the west coast and wide inland areas being perennially
123 subject to westerly moisture. These two major systems play significant roles in global climate
124 systems (Li et al., 2022; Wang et al., 2010). Moreover, the interactions across multiple heat
125 zones with sea and land provide conditions conducive to a wide variety of climate types. The
126 uplift of the Qinghai-Tibet plateau not only alters the climate patterns dominated by the
127 planetary wind system on the Eurasian continent and the moisture movement paths in the
128 Indian Ocean (An et al., 2001) but also changes the natural surface conditions, such as the
129 numerous rivers including the Yangtze, Yellow, Ganges, and Mekong Rivers, which play a
130 vital role in hydrological processes and human life. The plateau itself forms a relatively
131 complete vertical ecological environment differentiation, enhancing the complexity of the
132 natural environment on the Eurasian continent. Therefore, the research data and studies on
133 climate environmental changes in Eurasia hold significant representativeness in addressing
134 global changes.



135

136 **Fig.1** Distribution map of precipitation stable isotope sampling sites in the Eurasian continent

137

138 **3. Data and methodology**

139 **3.1 Data sources and collection**

140 We have collected $\delta^{18}\text{O}$ and $\delta^2\text{H}$ stable isotope data from precipitation at 1,930 s
141 ampling points across the Eurasian continent from 1961 to 2022. The dataset includes
142 both measured data and data collected from various sources. The collected data mainly
143 come from the Global Network of Isotopes in Precipitation (GNIP) and the Water Is
144 otopre Network operated by the International Atomic Energy Agency (IAEA) ([https://wa
145 teriso.utah.edu/waterisotopes/index.html](https://wateriso.utah.edu/waterisotopes/index.html)). In this study, we have compiled a total of 45,
146 782 data records, including 3,676 records from literature sources. The measured data
147 were collected, analyzed, and organized at the Shiyang River Basin Integrated Observa
148 tion Station of Northwest Normal University in China, comprising 2,297 data records.
149 Additionally, meteorological data used in this study are from the CRU TS v. 4.07 dat
150 aaset (Harris et al., 2020) and the NCEP-NCAR Reanalysis 1 dataset ([https://psl.noaa.go
151 v/data/gridded/data.ncep.reanalysis.html](https://psl.noaa.gov/data/gridded/data.ncep.reanalysis.html)).

152 **3.2 Data processing steps and quality control**



153 Data Collection: The data collected includes a variety of issues such as missing values,
154 outliers, and duplicates, as well as gaps in dates and missing or incorrect latitude and
155 longitude information. Therefore, the collected raw data underwent preprocessing and data
156 cleaning. Missing data was interpolated, entries that could not be completed were removed,
157 and duplicate data was eliminated.

158 Measured Data: Standard rain gauges were used to collect precipitation samples. After
159 each precipitation event, the collected samples were immediately transferred into 100ml
160 high-density sample bottles. To prevent data errors caused by evaporation, the collected water
161 samples were stored in a refrigerator at a temperature of approximately 4°C. Prior to analysis,
162 the precipitation samples were naturally thawed at room temperature. Impurities were filtered
163 out using a 0.45µm filter membrane, and the samples were transferred to 2ml sample bottles.
164 Isotope values were measured using a liquid water isotope analyzer (DLT-100, Los Gatos
165 Research, USA). For any abnormal or values that did not pass the LWIA post-analysis
166 software check, parallel samples were selected for re-measurement to ensure data accuracy
167 (Zhu et al., 2022). The isotopic abundances of ¹⁸O and ²H were expressed using the δ notation
168 relative to the International Atomic Energy Agency (IAEA) Vienna Standard Mean Ocean
169 Water (V-SMOW) reference, following the equation:

170
$$\delta_{\text{sample}} (\text{‰}) = \left[\frac{R_{\text{sample}}}{R_{V\text{-}smow}} - 1 \right] \times 1000$$

171 Here, R represents the ratio of the heavier isotope to the lighter isotope (i.e., ¹⁸O/¹⁶O or
172 ²H/¹H). We used the International Atomic Energy Agency (IAEA) standard (V-SMOW2) to
173 validate our isotope measurements, ensuring comparability between isotopic measurements
174 across laboratories and instruments.

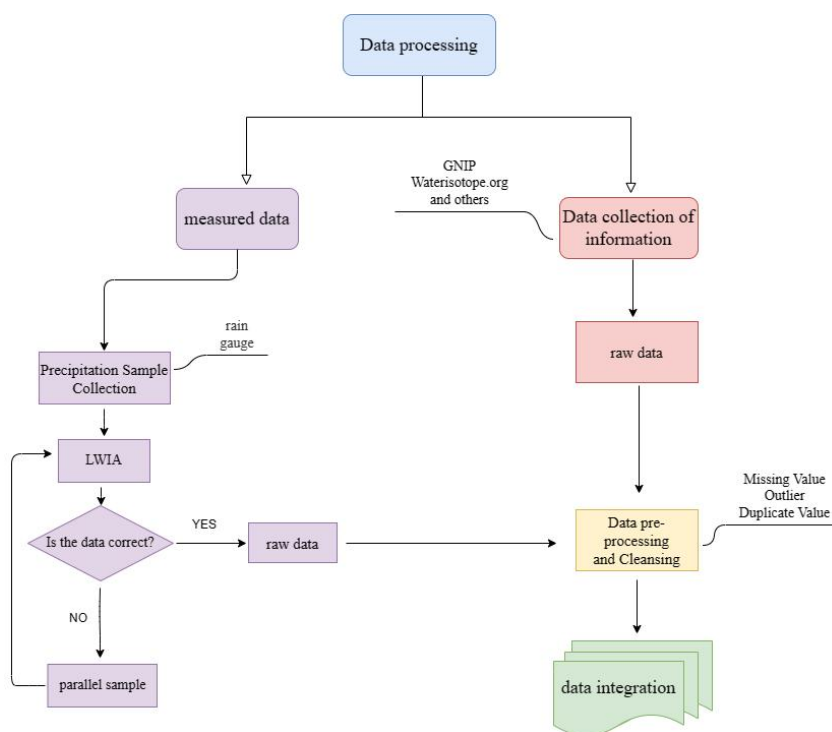
175 In 1982, Ferronsky VI and Polyakov VA conducted a study that found a general
176 distribution of δ¹⁸O and δ²H values in natural substances, indicating that the range of stable
177 isotope values for hydrogen and oxygen in atmospheric precipitation is typically -400‰ to
178 -30‰ and -60‰ to 10‰, respectively (Ferronsky VI et al., 1982). After data processing, the
179 data generally falls within the reasonable range.

180 Furthermore, the data has also undergone normality testing, the Mann-Kendall trend test,
181 and change point detection. The results of the Kolmogorov-Smirnov (K-S) test, which



182 examines the goodness of fit by comparing observed frequencies with expected frequencies,
183 are not significant, indicating that the data does not strictly follow a normal distribution.
184 However, the histogram of the data distribution and measures of skewness and kurtosis
185 suggest that the data approximately follows a normal distribution. The Mann-Kendall trend
186 test indicates an overall upward trend in the data over the long-term time series. Additionally,
187 the UFK-UBK curve exceeds the 95% confidence interval, indicating that the trend test is not
188 significant. This is mainly due to the increased seasonality and variability of stable isotopes in
189 precipitation, which contribute to the data's non-stationarity. The Mann-Kendall change point
190 test detected three significant change points.

191



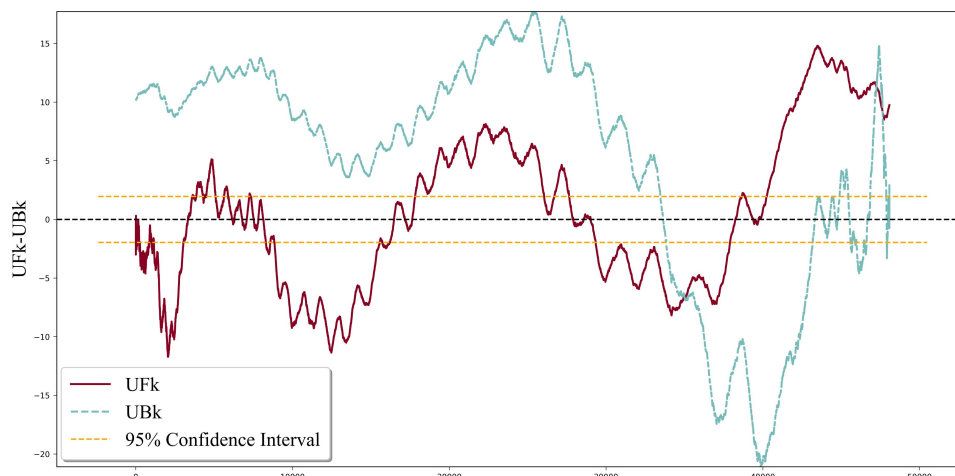
192

193

194

195

Fig.2 Flowchart of precipitation stable isotope dataset construction



196

197

Fig.3 The Mann-Kendall (MK) test for time series analysis.

198

199 **4. Results and discussion**

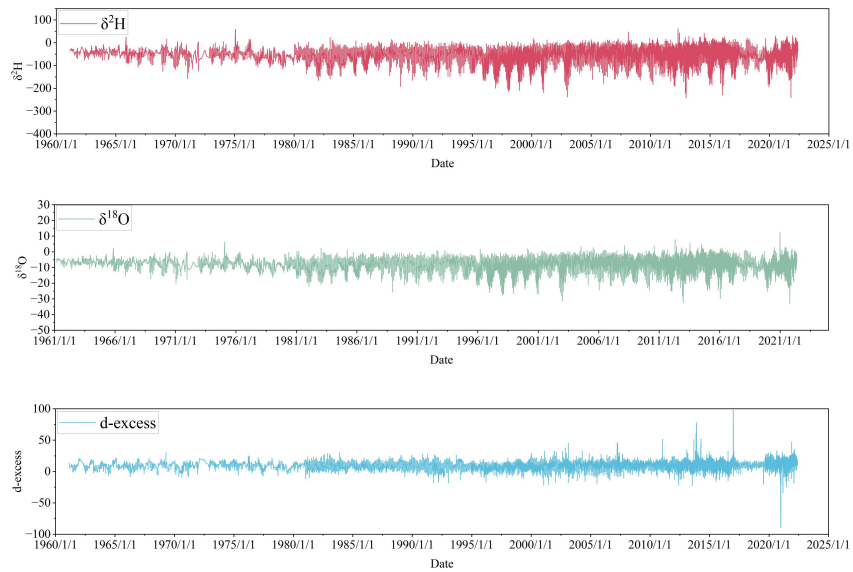
200 4.1 Temporal and Spatial Variation Characteristics of Precipitation Stable Isotopes

201 The hydrogen and oxygen stable isotopes in precipitation on the Eurasian continent
202 range from -332.4‰ to 62.05‰ and -41.4‰ to 23.18‰, respectively. The lower values of
203 stable isotopes reflect both high-altitude and high-latitude regions in terms of spatial
204 distribution. On a temporal scale, they also exhibit seasonal differences, with higher values in
205 summer and lower values in winter (Fig.4). The stable isotopes in precipitation on the
206 Eurasian continent show fluctuations influenced by seasonal factors. Since the 1960s, extreme
207 values of stable isotopes in precipitation have increased over time, indicating the
208 intensification of instability in meteorological elements such as temperature and precipitation.
209 This trend also suggests that the climate environment in the Eurasian continent is
210 experiencing an increase in extreme events under the backdrop of global change. As we face a
211 changing climate environment, the arid region of Central Asia has undergone a warming and
212 moistening process since the 1990s. This is characterized by increasing temperatures and
213 precipitation in the arid region, and even the occurrence of intense floods (Wei et al., 2023).
214 The response of stable isotopes in precipitation to extreme weather events is evident. For
215 example, stable isotopes in precipitation can explain the origin and intensification of extreme
216 rainfall events in Mumbai (Ansari et al., 2020). Stable isotopes in precipitation can detect



217 changes in climate and weather anomalies, providing us with valuable information in
218 long-term climate research.

219 From a spatial perspective, the stable isotopes in precipitation on the Eurasian continent
220 are influenced by an "elevation effect". The hydrogen and oxygen stable isotope values
221 gradually decrease from low to high latitudes (Fig.5). The multi-year average values of $\delta^2\text{H}$
222 and $\delta^{18}\text{O}$ at different latitudes are as follows: from 0°N to 30°N , -30.20‰ and -5.99‰ , from
223 30°N to 60°N , -58.94‰ and -8.77‰ , and from 60°N to 90°N , -92.98‰ and -12.69‰ .
224 Temperature is the dominant factor influencing the variations in stable isotopes in
225 precipitation on the Eurasian continent. In Southeast Asia, which is influenced by tropical
226 rainforest and monsoon climates, the high temperatures and humidity enhance the
227 "precipitation effect" on stable isotopes. In contrast, regions such as the Arabian Peninsula
228 and Central Asia, under desert climate conditions, experience high temperatures and low
229 rainfall, leading to enhanced evaporative fractionation and the "sub-cloud evaporation" effect,
230 resulting in larger values of stable isotopes in precipitation (Zhu et al., 2021). Additionally,
231 low values of stable isotopes in precipitation are observed in the Qinghai-Tibet Plateau and
232 the Alps in the mid-latitude regions. Overall, these variations are still influenced by
233 temperature. The spatial distribution of topographic features also affects the composition of
234 stable isotopes in precipitation. Compared to regions at the same latitude, the high values of
235 stable isotopes in precipitation extend to higher latitudes along the western coast of the
236 Eurasian continent, indicating higher temperatures in most parts of Europe at the same
237 latitude, especially in coastal areas near the North Pacific. Both regional and global water
238 cycles follow the principle of water balance. With increasing temperatures, the "low-value
239 zones" of stable isotopes in precipitation at high latitudes and altitudes will be more strongly
240 influenced. The substantial reduction of Arctic sea ice is a well-known climate change event
241 (Ding et al., 2017). Additionally, vegetation transpiration and water evaporation will enhance
242 atmospheric water vapour content. The impacts of these changes will be multifaceted,
243 potentially alleviating drought conditions in some regions while intensifying extreme
244 precipitation events, leading to severe climate disasters.



245

246

Fig.4 The time series variations of $\delta^2\text{H}$, $\delta^{18}\text{O}$, and d-excess in the Eurasian continent.

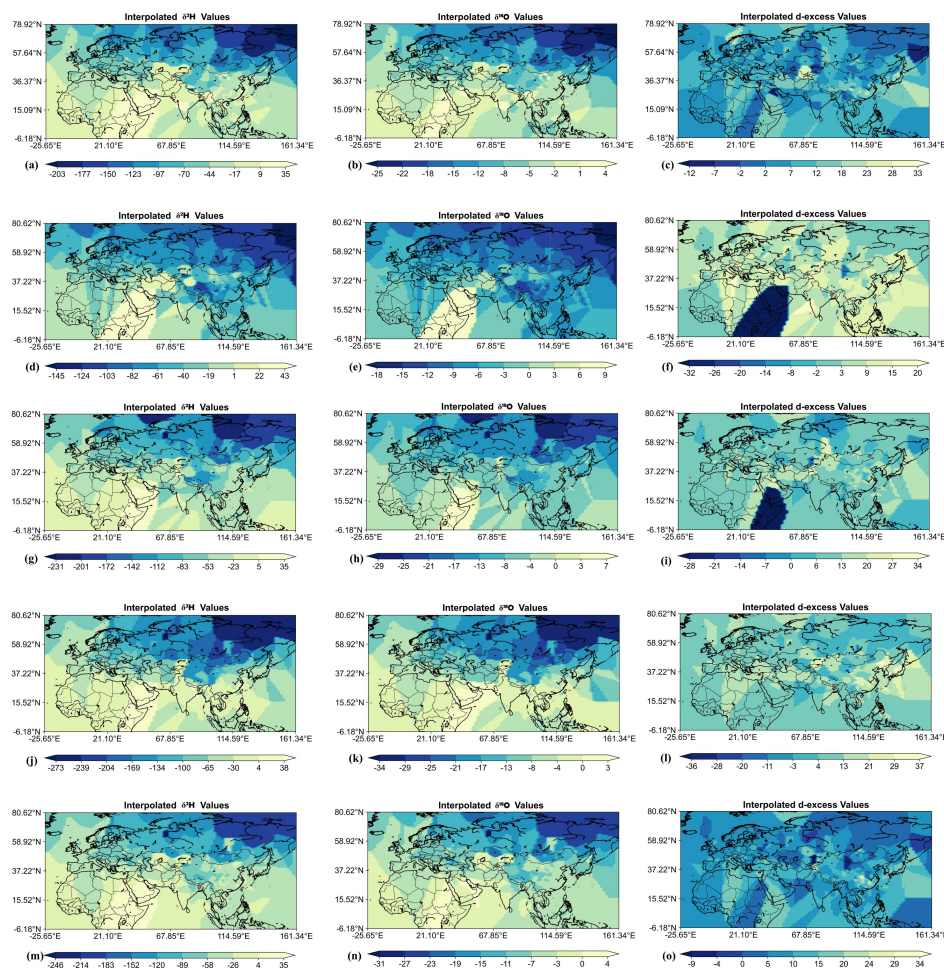


Fig.5 The spatial variations of $\delta^2\text{H}$, $\delta^{18}\text{O}$, and d-excess in the Eurasian continent. Panels (a), (b), and (c) display the spatial distribution of isotope values in the spring season. Panels (d), (e), and (f) show the spatial distribution of isotope values in the summer season. Panels (g), (h), and (i) present the spatial distribution of isotope values in the autumn season. Panels (j), (k), and (l) exhibit the spatial distribution of isotope values in the winter season. Panels (m), (n), and (o) display the spatial distribution of isotope values averaged over multiple years.

247

248 4.2 Seasonal changes in atmospheric precipitation lines and precipitation stable isotopes

249 The temporal and spatial variations of stable isotopes in precipitation are significantly
 250 influenced by meteorological factors, showing a high level of consistency with the climate
 251 regions they are in. Therefore, we classified the 12 climate zones in Eurasia according to the

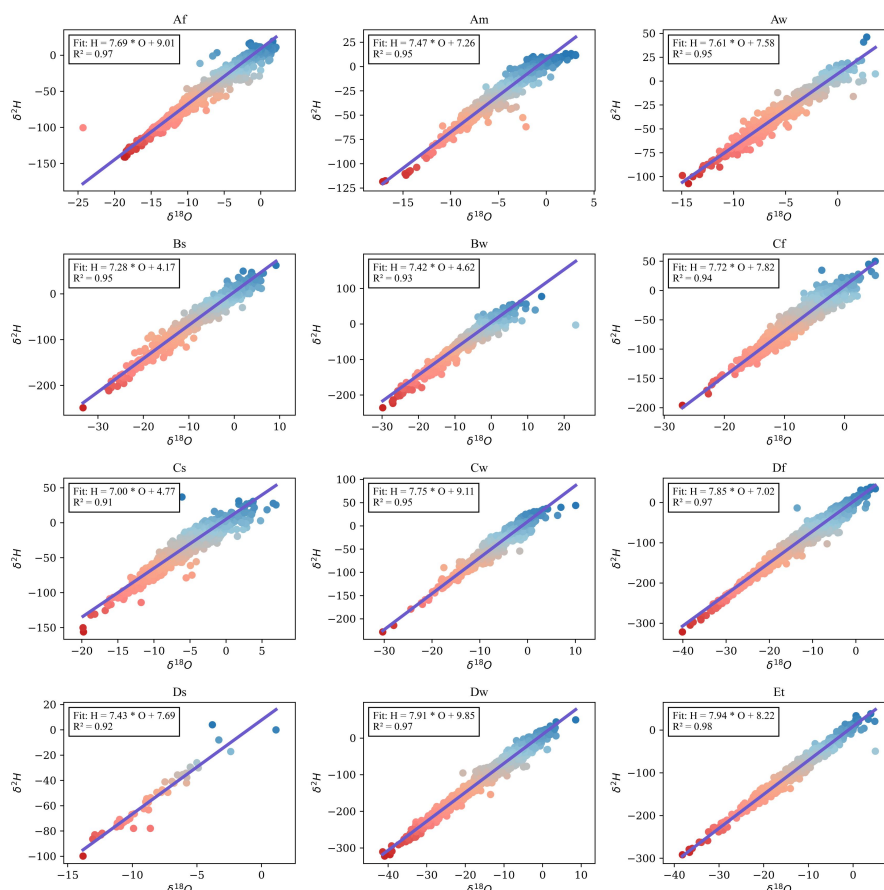


252 Köppen climate classification and used the least squares method to fit the atmospheric
253 precipitation lines (Fig.6). Köppen initially divided the world into five climate zones, with
254 four of them based on temperature (Beck, H.E., et al., 2018). These include the equatorial
255 climate zone (represented by A), the warm-temperate climate zone (represented by C), the
256 cold-temperate climate zone (represented by D), and the polar climate zone (represented by E).
257 All arid regions were separately classified as a climate zone, known as the dry climate zone
258 (represented by B). The atmospheric precipitation lines for different climate types show that
259 the tropical climate in type A exhibits relatively small differences in precipitation compared to
260 other climate types. The variation in slope and intercept of the atmospheric water lines is
261 determined by the combined effects of precipitation amount and temperature, with convective
262 precipitation weakening the influence of temperature effects. Types B and C climates exhibit
263 lower slopes and intercepts in their atmospheric precipitation lines. Stable isotopes in arid
264 climates are influenced by secondary evaporation below the clouds, resulting in strong
265 fractionation processes and relatively enriched stable isotopes in precipitation. Under
266 temperate climate conditions, the differences in stable isotope composition among different
267 climate regions become greater. In the Mediterranean region, which is controlled by the Cs
268 climate (summer-dry, warm), the slope and intercept are the lowest, indicating that
269 temperature increase dominates the hydrogen and oxygen stable isotope fractionation in
270 precipitation, suggesting a tendency towards aridity in this region under long-term average
271 conditions. In polar climates, the atmospheric precipitation lines exhibit higher slopes and
272 intercepts. In the polar climate environment, the influence of unbalanced fractionation
273 processes after the condensation of water vapour within cloud systems is relatively small,
274 resulting in a slope that is closer to 8. The differences in stable isotopes of precipitation
275 among different climate types indicate the relationship between precipitation and temperature.
276 The characteristics of high temperatures and low rainfall create a dry atmospheric
277 environment, and enhanced evaporation leads to a lower slope due to increased unbalanced
278 fractionation processes.

279 The seasonal variation of hydrogen and oxygen stable isotopes in precipitation on the
280 Eurasian continent generally exhibits a pattern of higher values in summer and lower values
281 in winter (Fig.7). The d-excess, which represents the deviation of the deuterium excess from



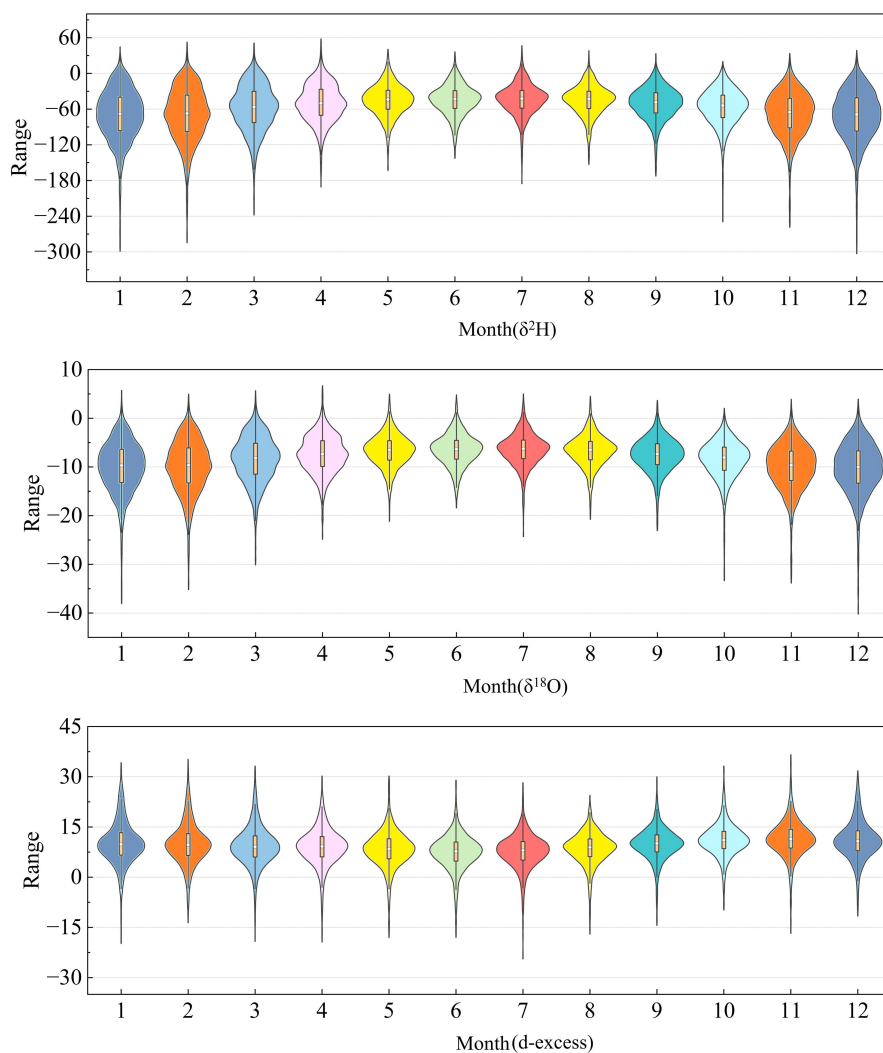
282 the global average, is lower in summer and higher in winter, indicating seasonal changes in
283 the source and transport distance of water vapor (Zhang et al., 2021). Furthermore, there are
284 regional differences in the seasonal variation of d-excess. This overall suggests that the
285 summer climate in the Eurasian continent is more humid, while the winter climate is drier.
286 However, the d-excess values, relative to $\delta^2\text{H}$ and $\delta^{18}\text{O}$, exhibit a more stable pattern and are
287 distributed around the global average. This indicates that the moisture in the vast regions of
288 the Eurasian continent is strongly influenced by oceanic water vapour. The state of the oceans
289 and large-scale atmospheric circulation changes can have a profound impact on the climate
290 environment of the Eurasian continent.



291
292 **Fig.6** Different atmospheric precipitation lines in various climate zones. The subgraph titles represent the
293 following climate zones: Af for Tropical Rainforest Climate, Am for Tropical Monsoon Climate, Aw for
294 Tropical Savanna Climate, Bs for Steppe Climate, Bw for Desert Climate, Cf for Temperate Oceanic
295 Climate, Cs for Mediterranean Climate, Cw for Humid Subtropical Climate, Df for Continental Subarctic



296 Climate, Ds for Subarctic Continental Climate, Dw for Subarctic Monsoon Climate, and Et for Tundra
297 Climate.
298



299
300 **Fig.7** Seasonal Distribution and Variations of Stable Isotopes in Precipitation

301 4.3 Drivers of stable isotope variation in precipitation in Asia and Europe

302 Meteorological variables accompany the fractionation process of stable hydrogen and
303 oxygen isotopes in precipitation, impacting the composition of stable isotopes (Sun et al.,
304 2019). We utilized a random forest regression model to assess the importance of

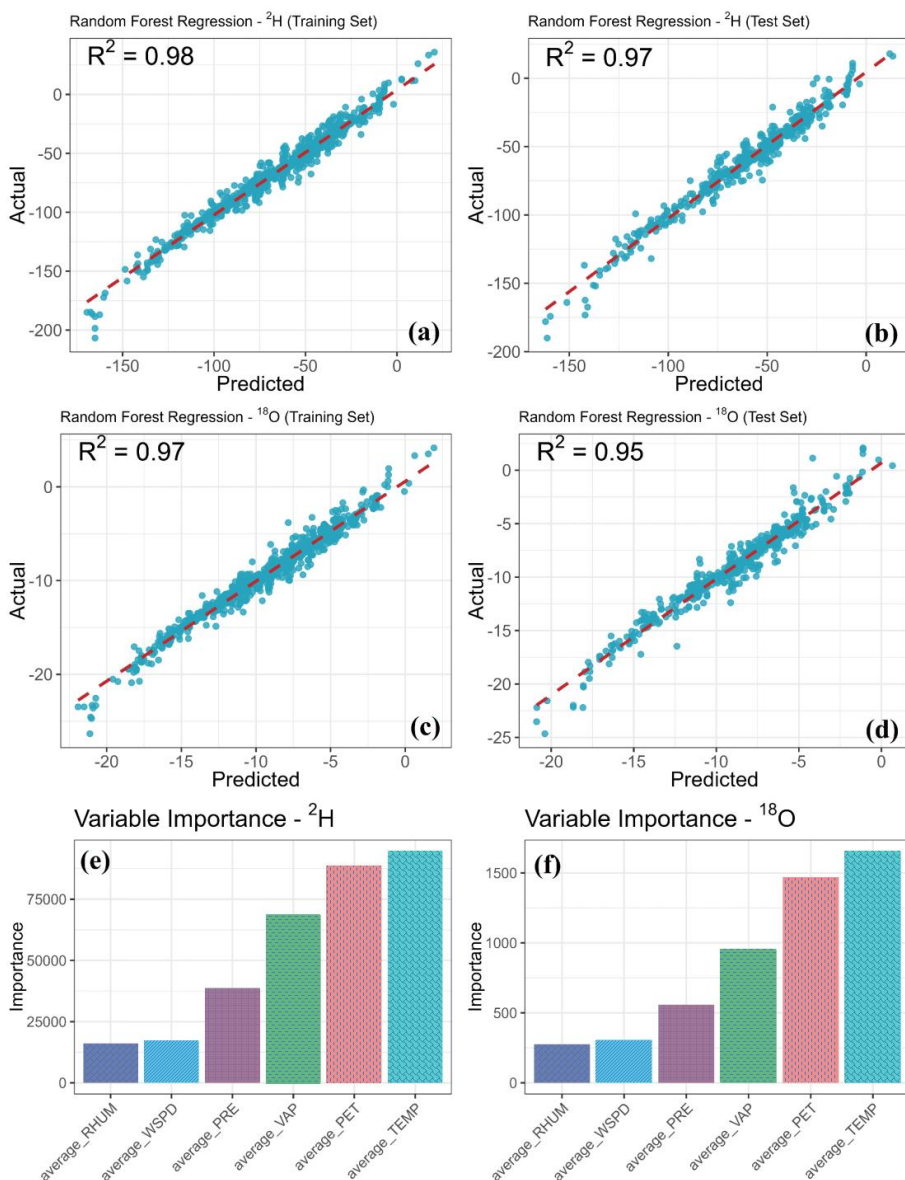


305 meteorological variables in the Eurasian continent on stable isotopes. Random forest
306 regression is a non-parametric method used to solve prediction problems. It predicts
307 regression problems based on the average results of random decision trees, which use
308 bootstrapping to eliminate the possibility of overfitting (Erdélyi et al., 2023). The random
309 forest regression analysis of the fitted stable isotopes of hydrogen and oxygen showed good
310 goodness of fit for both the training and testing sets, indicating that temperature, precipitation,
311 potential evapotranspiration, vapour pressure, wind speed, and relative humidity have a high
312 explanatory power for stable isotopes of hydrogen and oxygen (Fig.8). The composition of
313 stable isotopes in precipitation is greatly influenced by meteorological variables. However,
314 due to the spatial resolution of reanalysis meteorological data, the resampling process of
315 meteorological variables increased the repetition values, resulting in an improved variance
316 explanation rate for the dependent variable. Among the six variables considered, temperature
317 has the strongest explanatory power for the variation of stable isotopes of hydrogen and
318 oxygen, and potential evapotranspiration also has a relatively strong explanatory ability,
319 indicating that temperature change primarily drives the variation of stable isotopes in
320 precipitation in the Eurasian continent. The relative humidity is the ratio of actual vapour
321 pressure to saturated vapour pressure, but there is a significant difference in the explanatory
322 power of vapour pressure and relative humidity on stable isotopes. Vapour pressure has a
323 wider range of variation in the atmosphere, thus it may have greater variability in the
324 regression model, leading to a larger impact on predicting stable isotopes in precipitation.
325 Relative humidity, on the other hand, is a relative indicator with a relatively smaller range of
326 variation, so it may have a weaker predictive ability for stable isotopes in precipitation in the
327 regression model. The driving factors for the variation of stable isotopes in precipitation in the
328 Eurasian continent include climate change, seasonal variations, topography and landforms, as
329 well as water cycle processes, which collectively influence the isotopic composition of
330 precipitation. Atmospheric circulation directly affects the source of water vapor and the path
331 of moisture, while other factors primarily influence the composition of stable isotopes in
332 precipitation by altering temperature. For example, potential evapotranspiration plays a
333 crucial role in explaining the variation of stable isotopes in precipitation. However, the control
334 of meteorological variables on stable isotopes in precipitation varies between regions. Studies



335 on two precipitation stations in Crimea have shown weak correlations between temperature,
336 precipitation, and stable isotopes in precipitation. The complex natural environment
337 determines that no single factor has a dominant control over the stable isotopes in
338 precipitation in that region, and the composition of stable isotopes in precipitation is
339 influenced by both local and distant factors (Dublyansky et al., 2018). In the eastern coastal
340 region of China, the relative enrichment of stable isotopes in precipitation is due to the
341 proximity to the evaporative source of the ocean, leading to an increased abundance of heavy
342 isotopes (Zhang et al., 2021). In the arid region of central Asia, there is a strong correlation
343 between stable isotopes in precipitation and temperature, and the enrichment or depletion of
344 stable isotopes in precipitation reflects the trend of temperature change (Zhu et al., 2023). In
345 summary, the meteorological control factors of the composition of stable isotopes in
346 precipitation vary in different regions. There is a strong relationship between stable isotopes
347 in precipitation and meteorological variables, and stable hydrogen and oxygen isotopes may
348 be considered essential climate response variables, which will contribute to describing the
349 hydrological cycle and better predicting the response of future climate change and ecosystem
350 changes.

351



352

353

354

355

356

357

358

359

Fig.8 Results of Random Forest Regression Analysis for $\delta^2\text{H}$ and $\delta^{18}\text{O}$ in Relation to Meteorological Variables. a: Regression results for the training set of $\delta^2\text{H}$, b: Regression results for the testing set of $\delta^2\text{H}$, c: Regression results for the training set of $\delta^{18}\text{O}$, d: Regression results for the testing set of $\delta^{18}\text{O}$, e: Importance of meteorological variables for $\delta^2\text{H}$, f: Importance of meteorological variables for $\delta^{18}\text{O}$



360 **Data Availability**

361 Zhu, Guofeng (2023), “Dataset of Stable Isotopes of Precipitation in the Eurasian
362 Continent”, Mendeley Data, V1, doi: 10.17632/rbn35yrbd2.1

363 **Author contribution Statement**

364 Longhu Chen: Conceptualization and Writing-Original draft preparation; Qinqin Wang:
365 Writing and Data processing; Guofeng Zhu: Writing review and editing; Xinrui Lin:
366 Modification; Dongdong Qiu: Modification; Yinying Jiao: data processing; Siyu Lu:
367 Experiment; Rui Li: Methodology; Gaojia Meng: Visualization; Yuhao Wang: Visualization.

368 **Declaration of Interest Statement**

369 The authors declare that they have no known competing financial interests or personal
370 relationships that could have appeared to influence the work reported in this paper.

371 **Acknowledgements**

372 This research was financially supported by the National Natural Science Foundatio
373 n of China(42371040, 41971036), Key Natural Science Foundation of Gansu Province
374 (23JRRA698), Key Research and Development Program of Gansu Province(22YF7NA1
375 22), Cultivation Program of Major key projects of Northwest Normal University(NWN
376 U-LKZD-202302), Oasis Scientific Research achievements Breakthrough Action Plan Pr
377 oject of Northwest Normal University(NWNU-LZKX-202303). The authors thank their
378 Northwest Normal University colleagues for their help in fieldwork, laboratory analysis,
379 and data processing.

380 **Reference**

- 381 Ansari, Md. A., Noble, J., Deodhar, A., Mendhekar, G. N., and Jahan, D.: Stable isotopic ($\delta^{18}\text{O}$ an
382 d $\delta^2\text{H}$) and geospatial approach for evaluating extreme rainfall events, *Glob. Planet. Change*, 1
383 94, 103299, <https://doi.org/10.1016/j.gloplacha.2020.103299>, 2020.
- 384 Beck, H. E., Zimmermann, N. E., McVicar, T. R., Vergopolan, N., Berg, A., and Wood, E. F.: Pre
385 sent and future Köppen-Geiger climate classification maps at 1-km resolution, *Sci. Data*, 5, 18
386 0214, <https://doi.org/10.1038/sdata.2018.214>, 2018.
- 387 Bowen, G. J., Cai, Z., Fiorella, R. P., and Putman, A. L.: Isotopes in the Water Cycle: Regional-
388 to Global-Scale Patterns and Applications, *Annu. Rev. Earth Planet. Sci.*, 47, 453–479, <https://doi.org/10.1146/annurev-earth-053018-060220>, 2019.



- 390 Caley, T., Roche, D. M., and Renssen, H.: Orbital Asian summer monsoon dynamics revealed using
391 an isotope-enabled global climate model, *Nat. Commun.*, 5, 5371, <https://doi.org/10.1038/ncomms6371>, 2014.
- 392
- 393 Craig, H.: Isotopic Variations in Meteoric Waters, *Sci. New Ser.*, 133, 1702–1703, 1961.
- 394 Czuppon, G., Bottyán, E., Kristóf, E., Weidinger, T., Haszpra, L., and Kármán, K.: Stable isotope
395 data of daily precipitation during the period of 2013–2017 from K-puszta (regional background
396 monitoring station), Hungary, *Data Brief*, 36, 106962, <https://doi.org/10.1016/j.dib.2021.106962>,
397 2021.
- 398 Dansgaard, W.: Stable isotopes in precipitation, *Tellus*, 16, 436–468, [https://doi.org/10.3402/tellusa.v](https://doi.org/10.3402/tellusa.v16i4.8993)
399 16i4.8993, 1964.
- 400 Delavau, C. J., Stadnyk, T., and Holmes, T.: Examining the impacts of precipitation isotope input
401 ($\delta^{18}\text{O}_{\text{ppt}}$) on distributed, tracer-aided hydrological modelling, *Hydrol. Earth Syst. Sci.*, 21, 2595
402 –2614, <https://doi.org/10.5194/hess-21-2595-2017>, 2017.
- 403 Ding, Q., Schweiger, A., L'Heureux, M., Battisti, D. S., Po-Chedley, S., Johnson, N. C., Blanchard
404 -Wrigglesworth, E., Harnos, K., Zhang, Q., Eastman, R., and Steig, E. J.: Influence of high-latitude
405 atmospheric circulation changes on summertime Arctic sea ice, *Nat. Clim. Change*, 7, 28
406 9–295, <https://doi.org/10.1038/nclimate3241>, 2017.
- 407 Dublyansky, Y. V., Klimchouk, A. B., Tokarev, S. V., Amelichev, G. N., Langhamer, L., and Spötl,
408 C.: Stable isotopic composition of atmospheric precipitation on the Crimean Peninsula and its
409 controlling factors, *J. Hydrol.*, 565, 61–73, <https://doi.org/10.1016/j.jhydrol.2018.08.006>, 2018.
- 410 Eastoe, C. J. and Dettman, D. L.: Isotope amount effects in hydrologic and climate reconstructions
411 of monsoon climates: Implications of some long-term data sets for precipitation, *Chem. Geol.*,
412 430, 78–89, <https://doi.org/10.1016/j.chemgeo.2016.03.022>, 2016.
- 413 Erdélyi, D., Hatvani, I. G., Jeon, H., Jones, M., Tyler, J., and Kern, Z.: Predicting spatial distribution
414 of stable isotopes in precipitation by classical geostatistical- and machine learning methods,
415 *J. Hydrol.*, 617, 129129, <https://doi.org/10.1016/j.jhydrol.2023.129129>, 2023.
- 416 Faranda, D., Messori, G., Jezequel, A., and Vrac, M.: Atmospheric circulation compounds anthropo
417 genic warming and impacts of climate extremes in Europe, *Proc. Natl. Acad. Sci.*, 120, e2214
418 525120, <https://doi.org/10.1073/pnas.2214525120>, 2023.
- 419 Gat, J. R.: OXYGEN AND HYDROGEN ISOTOPES IN THE HYDROLOGIC CYCLE, 1996.



- 420 Gou, J., Qu, S., Guan, H., Shi, P., Su, Z., Lin, Z., Liu, J., and Zhu, J.: Relationship between precipi-
421 tation isotopic compositions and synoptic atmospheric circulation patterns in the lower reach
422 of the Yangtze River, *J. Hydrol.*, 605, 127289, <https://doi.org/10.1016/j.jhydrol.2021.127289>, 2
423 022.
- 424 Harris, I., Osborn, T. J., Jones, P., and Lister, D.: Version 4 of the CRU TS monthly high-resoluti-
425 on gridded multivariate climate dataset, *Sci. Data*, 7, 109, <https://doi.org/10.1038/s41597-020-04>
426 53-3, 2020.
- 427 Jiao, Y., Liu, C., Liu, Z., Ding, Y., and Xu, Q.: Impacts of moisture sources on the temporal and
428 spatial heterogeneity of monsoon precipitation isotopic altitude effects, *J. Hydrol.*, 583, 124576,
429 <https://doi.org/10.1016/j.jhydrol.2020.124576>, 2020.
- 430 Li, G., Wang, X., Zhang, X., Yan, Z., Liu, Y., Yang, H., Wang, Y., Jonell, T. N., Qian, J., Gou,
431 S., Yu, L., Wang, Z., and Chen, J.: Westerlies-Monsoon interaction drives out-of-phase precipit-
432 ation and asynchronous lake level changes between Central and East Asia over the last millen-
433 nium, *CATENA*, 218, 106568, <https://doi.org/10.1016/j.catena.2022.106568>, 2022.
- 434 Liu, Y., Cai, W., Lin, X., and Li, Z.: Increased extreme swings of Atlantic intertropical convergenc-
435 e zone in a warming climate, *Nat. Clim. Change*, 12, 828–833, <https://doi.org/10.1038/s41558->
436 022-01445-y, 2022.
- 437 Ma, F., Chen, J., Chen, J., and Wang, T.: Environmental drivers of precipitation stable isotopes an-
438 d moisture sources in the Mongolian Plateau, *J. Hydrol.*, 621, 129615, <https://doi.org/10.1016/j>.
439 [j.jhydrol.2023.129615](https://doi.org/10.1016/j.jhydrol.2023.129615), 2023.
- 440 Nan, Y., He, Z., Tian, F., Wei, Z., and Tian, L.: Can we use precipitation isotope outputs of isoto-
441 pic general circulation models to improve hydrological modeling in large mountainous catchme-
442 nts on the Tibetan Plateau?, *Hydrol. Earth Syst. Sci.*, 25, 6151–6172, <https://doi.org/10.5194/he>
443 [ss-25-6151-2021](https://doi.org/10.5194/ess-25-6151-2021), 2021.
- 444 Natali, S., Baneschi, I., Doveri, M., Gianecchini, R., Selmo, E., and Zanchetta, G.: Meteorological
445 and geographical control on stable isotopic signature of precipitation in a western Mediterran-
446 ean area (Tuscany, Italy): Disentangling a complex signal, *J. Hydrol.*, 603, 126944, <https://doi>.
447 [org/10.1016/j.jhydrol.2021.126944](https://doi.org/10.1016/j.jhydrol.2021.126944), 2021.
- 448 Nelson, D. B., Basler, D., and Kahmen, A.: Precipitation isotope time series predictions from mach-
449 ine learning applied in Europe, *Proc. Natl. Acad. Sci.*, 118, e2024107118, <https://doi.org/10.107>



- 450 3/pnas.2024107118, 2021.
- 451 Ruan, J., Zhang, H., Cai, Z., Yang, X., and Yin, J.: Regional controls on daily to interannual varia
452 tions of precipitation isotope ratios in Southeast China: Implications for paleomonsoon reconstr
453 uction, *Earth Planet. Sci. Lett.*, 527, 115794, <https://doi.org/10.1016/j.epsl.2019.115794>, 2019.
- 454 Shi, M., Worden, J. R., Bailey, A., Noone, D., Risi, C., Fu, R., Worden, S., Herman, R., Payne,
455 V., Pagano, T., Bowman, K., Bloom, A. A., Saatchi, S., Liu, J., and Fisher, J. B.: Amazonian
456 terrestrial water balance inferred from satellite-observed water vapor isotopes, *Nat. Commun.*,
457 13, 2686, <https://doi.org/10.1038/s41467-022-30317-4>, 2022.
- 458 Shi, Y., Wang, S., Wang, L., Zhang, M., Argiriou, A. A., Song, Y., and Lei, S.: Isotopic evidence
459 in modern precipitation for the westerly meridional movement in Central Asia, *Atmospheric Re*
460 *s.*, 259, 105698, <https://doi.org/10.1016/j.atmosres.2021.105698>, 2021.
- 461 Sun, C., Chen, Y., Li, J., Chen, W., and Li, X.: Stable isotope variations in precipitation in the no
462 rthwesternmost Tibetan Plateau related to various meteorological controlling factors, *Atmospheri*
463 *c Res.*, 227, 66–78, <https://doi.org/10.1016/j.atmosres.2019.04.026>, 2019.
- 464 V.I. Ferronisky and V.A. Polyakov, P. (Eds.): *Isotopes of the Earth's Hydrosphere*, Springer Publicati
465 ons, ISBN: 978-94-007-2855-4, 2012.
- 466 Wang, S., Lei, S., Zhang, M., Hughes, C., Crawford, J., Liu, Z., and Qu, D.: Spatial and Seasonal
467 Isotope Variability in Precipitation across China: Monthly Isoscapes Based on Regionalized F
468 uzzy Clustering, *J. Clim.*, 35, 3411–3425, <https://doi.org/10.1175/JCLI-D-21-0451.1>, 2022.
- 469 Wang, Y., Liu, X., and Herzschuh, U.: Asynchronous evolution of the Indian and East Asian Sum
470 mer Monsoon indicated by Holocene moisture patterns in monsoonal central Asia, *Earth-Sci. R*
471 *ev.*, 103, 135–153, <https://doi.org/10.1016/j.earscirev.2010.09.004>, 2010.
- 472 Wei, W., Zou, S., Duan, W., Chen, Y., Li, S., and Zhou, Y.: Spatiotemporal variability in extreme
473 precipitation and associated large-scale climate mechanisms in Central Asia from 1950 to 2019,
474 *J. Hydrol.*, 620, 129417, <https://doi.org/10.1016/j.jhydrol.2023.129417>, 2023.
- 475 Wei, Z., Lee, X., Aemisegger, F., Benetti, M., Berkelhammer, M., Casado, M., Caylor, K., Christne
476 r, E., Dyroff, C., García, O., González, Y., Griffis, T., Kurita, N., Liang, J., Liang, M.-C., Lin,
477 G., Noone, D., Griбанov, K., Munksgaard, N. C., Schneider, M., Ritter, F., Steen-Larsen, H.
478 C., Vallet-Coulomb, C., Wen, X., Wright, J. S., Xiao, W., and Yoshimura, K.: A global databa
479 se of water vapor isotopes measured with high temporal resolution infrared laser spectroscopy,



- 480 Sci. Data, 6, 180302, <https://doi.org/10.1038/sdata.2018.302>, 2019.
- 481 Yao, T., Masson-Delmotte, V., Gao, J., Yu, W., Yang, X., Risi, C., Sturm, C., Werner, M., Zhao,
482 H., He, Y., Ren, W., Tian, L., Shi, C., and Hou, S.: A review of climatic controls on $\delta^{18}\text{O}$ i
483 n precipitation over the Tibetan Plateau: Observations and simulations, *Rev. Geophys.*, 51, 525
484 –548, <https://doi.org/10.1002/rog.20023>, 2013.
- 485 Zhang, J., Yu, W., Jing, Z., Lewis, S., Xu, B., Ma, Y., Wei, F., Luo, L., and Qu, D.: Coupled Eff
486 ects of Moisture Transport Pathway and Convection on Stable Isotopes in Precipitation across
487 the East Asian Monsoon Region: Implications for Paleoclimate Reconstruction, *J. Clim.*, 1–41,
488 <https://doi.org/10.1175/JCLI-D-21-0271.1>, 2021.
- 489 Zhang, J., Chen, H., Nie, Y., Fu, Z., Lian, J., Luo, Z., and Wang, F.: Temporal variations of preci
490 pitation driven by local meteorological parameters in southwest China: Insights from 9 years o
491 f continuous hydro-meteorological and isotope observations, *J. Hydrol. Reg. Stud.*, 46, 101345,
492 <https://doi.org/10.1016/j.ejrh.2023.101345>, 2023.
- 493 Zhang, Q., Gu, X., Singh, V. P., Sun, P., Chen, X., and Kong, D.: Magnitude, frequency and timi
494 ng of floods in the Tarim River basin, China: Changes, causes and implications, *Glob. Planet.
495 Change*, 139, 44–55, <https://doi.org/10.1016/j.gloplacha.2015.10.005>, 2016.
- 496 Zhao, L., Dong, X., Liu, X., Wang, N., Eastoe, C. J., Wei, N., Xie, C., Liu, H., Han, C., Hua, T.,
497 and Wang, L.: Extreme precipitation stable isotopic compositions reveal unexpected summer
498 monsoon incursions in the Qilian Mountains, *Sci. Total Environ.*, 900, 165743, <https://doi.org/10.1016/j.scitotenv.2023.165743>, 2023.
- 500 Zhisheng, A., Kutzbach, J. E., Prell, W. L., and Porter, S. C.: Evolution of Asian monsoons and p
501 hased uplift of the Himalaya–Tibetan plateau since Late Miocene times, *Nature*, 411, 62–66, h
502 <https://doi.org/10.1038/35075035>, 2001.
- 503 Zhu, G., Guo, H., Qin, D., Pan, H., Zhang, Y., Jia, W., and Ma, X.: Contribution of recycled moi
504 sture to precipitation in the monsoon marginal zone: Estimate based on stable isotope data, *J.
505 Hydrol.*, 569, 423–435, <https://doi.org/10.1016/j.jhydrol.2018.12.014>, 2019.
- 506 Zhu, G., Zhang, Z., Guo, H., Zhang, Y., Yong, L., Wan, Q., Sun, Z., and Ma, H.: Below-Cloud E
507 vaporation of Precipitation Isotopes over Mountains, Oases, and Deserts in Arid Areas, *J. Hyd
508 rometeorol.*, 22, 2533–2545, <https://doi.org/10.1175/JHM-D-20-0170.1>, 2021.
- 509 Zhu, G., Liu, Y., Shi, P., Jia, W., Zhou, J., Liu, Y., Ma, X., Pan, H., Zhang, Y., Zhang, Z., Sun,



510 Z., Yong, L., and Zhao, K.: Stable water isotope monitoring network of different water bodies
511 in Shiyang River basin, a typical arid river in China, Earth Syst. Sci. Data, 14, 3773–3789,
512 <https://doi.org/10.5194/essd-14-3773-2022>, 2022.

513 Zhu, G., Liu, Y., Shi, P., Jia, W., Zhou, J., Liu, Y., Ma, X., Pan, H., Zhang, Y., Zhang, Z., Sun,
514 Z., Yong, L., and Zhao, K.: Stable water isotope monitoring network of different water bodies
515 in Shiyang River basin, a typical arid river in China, Earth Syst. Sci. Data, 14, 3773–3789,
516 <https://doi.org/10.5194/essd-14-3773-2022>, 2022.